JOURNAL OF GEOPHYSICAL RESEARCH, VOL. 106, NO. A12, PAGES 29,733–29,744, DECEMBER 1, 2001

Lightning-induced energetic electron flux enhancements in the drift loss cone

J. B. Blake,[1] U. S. Inan,[2] M. Walt,[2] T. F. Bell,[2] J. Bortnik,[2]
D. L. Chenette,[3] and H. J. Christian[4]

Abstract. With its relatively low altitude (520 × 670 km) orbit, SAMPEX is mostly below the stable trapping region where charged particles repeatedly drift around the Earth, especially at midlatitudes. Recent analyses of SAMPEX data have revealed a surprisingly common set of observations of enhanced energetic (>150 keV) electron fluxes at $L < 3$, during times when SAMPEX was located such that any electrons that it observed were in the drift loss cone (and were thus destined to be precipitated upon reaching the longitude of the South Atlantic Magnetic Anomaly in the course of their eastward drift). The data were acquired with the Heavy Ion Large Telescope on board SAMPEX, which provides high time resolution measurements (30 ms sample rate) of electrons above energy thresholds of 150 keV and 1 MeV. Preliminary examination of 1995 SAMPEX data (when the >150 keV detector was available) revealed hundreds of cases of newly enhanced drift loss cone fluxes in localized L shell regions often associated with individual thunderstorms. In one case, SAMPEX data from three consecutive days (95/196, 95/197, and 95/198) were analyzed as the satellite proceeded northbound over the same ground track from west of New Zealand and Hawaii toward Alaska, with the underlying lightning activity documented by the Optical Transient Detector on board the OrbView-1 satellite (750 km, 70° inclination circular orbit). Enhanced fluxes observed on SAMPEX during day 95/197 were directly associated with an oceanic storm just to the west of the SAMPEX ground track, which was well placed to generate the observed drift loss cone flux enhancements. The drift loss cone electron flux enhancements were also observed 20 min later as SAMPEX crossed the same L shells in the north and in subsequent orbits, indicating that lightning-induced precipitation of electrons into the drift loss cone persisted at least for a few hours. Data from UARS satellite, passing through the same region within the same hour, also confirmed the presence of L-dependent structure and further allowed the determination of the electron energy spectra, which exhibited a general shape and range strikingly similar to previously documented spectral characteristics of lightning-induced electron precipitation (LEP) events in the bounce loss cone [*Voss et al*., 1998]. This similarity lends support to the argument that the observed drift loss cone features are produced by the LEP process. In summary, SAMPEX data indicate that globally distributed thunderstorms may continually precipitate energetic electrons from the radiation belts, producing transient enhancements in the drift loss cone that are detected within the few hour periods as they drift around the Earth and precipitate in the South Atlantic Magnetic Anomaly.

1. Introduction

The Stimulated Emissions of Energetic Particles (SEEP) investigation on the S81-1 spacecraft provided the first satellite measurements of lightning-induced electron precipitation (LEP) [*Voss et al*., 1984]. SEEP observed short bursts of electrons in the bounce loss cone [cf. *Roederer*, 1970], i.e., electrons that would have impinged upon the upper atmosphere within one bounce. Some of these electrons were backscattered from the atmosphere, leading to a series of peaks in electron intensity of steadily decreasing amplitude [*Voss et al*., 1998]; all were lost into the atmosphere within several bounces. The LEP events observed by SEEP consisted of peak fluxes of 10^4 electrons/cm^2 sr s in ~1-s bursts of ~100–300 keV electrons.

LEP bursts in the bounce loss cone also can be detected from the ground via the associated D region ionisation registered as subionospheric VLF signal perturbations, with individual LEP bursts unambiguously associated with causative lightning discharges [e.g., *Inan et al*., 1988a]. Such measurements indicate that tens to hundreds of LEP events can be produced by a single thunderstorm [e.g., *Inan et al*., 1988b, 1990; *Lev-Tov et al*., 1995]. Formerly, LEP events were thought to be produced only by ducted whistlers, which propagate within (and thus affect only the electrons within) filamentary ducts <400 km in diameter at the equator [e.g., *Burgess and Inan*, 1993]. Recently, in a juxtaposition of theoretical predic-

[1]Space Sciences Department, The Aerospace Corporation, Los Angeles, California, USA.
[2]Electrical Engineering Department, Stanford University, Stanford, California, USA.
[3]Lockheed Martin Advanced Technology Center (LMATC), Palo Alto, California, USA.
[4]NASA/Marshall Space Flight Center, Huntsville, Alabama, USA.

Paper number 2001JA000067.
0148-0227/01/2001JA000067$09.00

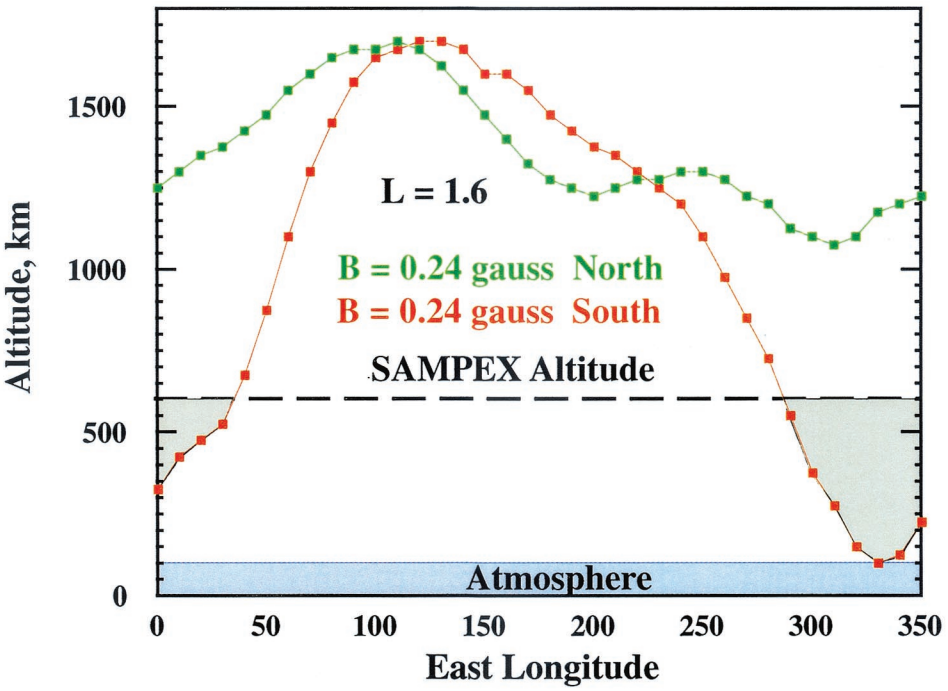

Plate 1. Altitude of the $B = 0.24$ G point is shown as a function of longitude for both the Northern and Southern Hemispheres. Note that the altitude drops to 100 km in the Southern Hemisphere in the South Atlantic Magnetic Anomaly (SAA).

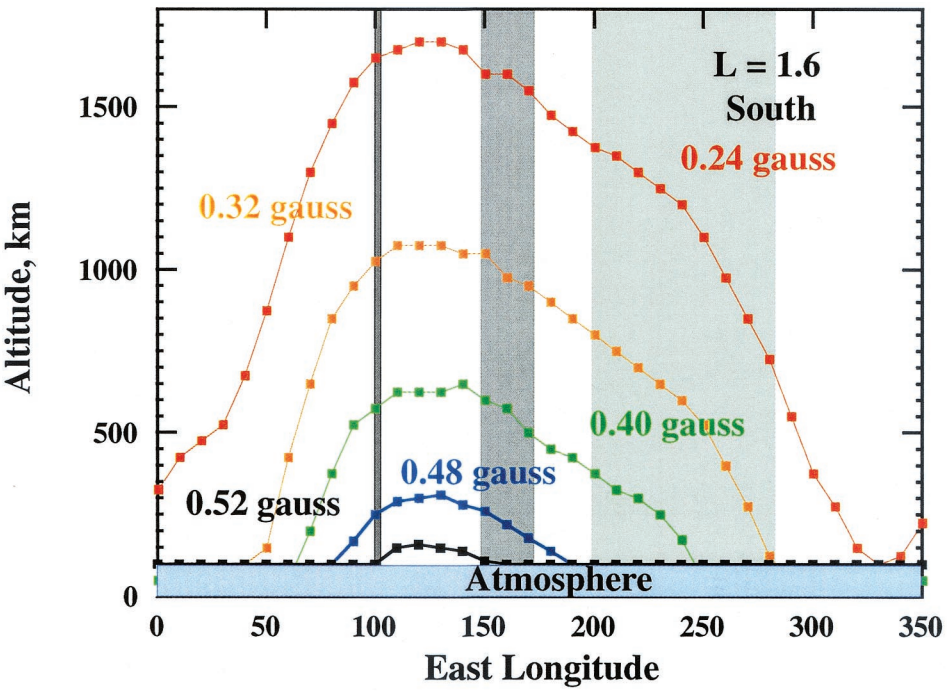

Plate 2. Altitude of the locus of constant B as a function of longitude is plotted for several magnetic field values ranging from 0.24 to 0.52 G. Also shown schematically is how an LEP at 100° longitude would spread out due to energy-dependent drift speed as the LEP electrons drift eastward toward the SAA.

tion [*Lauben et al*., 1999] and experimental observation [*Johnson et al*., 1999], imaging of the associated ionospheric disturbance using multiple closely spaced VLF paths has revealed that individual lightning flashes can precipitate significant fluxes of energetic electrons ($>10^{-5}$ ergs/cm^2 s) over an ionospheric region of ~2000-km horizontal extent. The electromagnetic energy originating in lightning discharges propagates to large distances in the Earth-ionosphere waveguide, continually leaking up to the magnetosphere, propagating as oblique (nonducted) whistler waves therein, and pitch angle scattering (and thus precipitating) energetic electrons. The experimental observation by *Johnson et al*. [1999] of the specific theoretical predictions (including the latitudinal dependence of temporal signatures) of *Lauben et al*. [1999] clearly demonstrated that LEP events can be produced by nonducted whistlers launched by lightning.

In this paper, we report new observations of LEP events seen in the drift loss cone [cf. *Roederer*, 1970] with energetic particle sensors on board the SAMPEX and UARS satellites. At times, extensive precipitation into the drift loss cone, and perforce the bounce loss cone, persists for many hours and perhaps for a day or more, suggesting that lightning-induced precipitation may be a significant factor controlling the lifetime of energetic electrons in the inner belt and slot regions.

2. Satellites and Instrumentation

SAMPEX was launched on July 3, 1992, into a 520 × 670 km orbit with an inclination of 82°. Energetic electron data were acquired by SAMPEX with the Heavy Ion Large Telescope (HILT) [*Klecker et al*., 1993]. Although HILT was designed to measure heavy ions in the range from 4 to 250 MeV/nucleon by means of multiple coincidences and pulse-height analyses, single detector rates provided high time resolution measurements (30 ms sample rate) of electrons above two energy thresholds of 150 keV and 1 MeV. The HILT instrument has a large geometric factor (~80 cm^2 sr) and a broad field of view, ~45° half angle. Thus, even when the sensor central axis was directed normal to the magnetic field, much of the instrument solid angle was well away from the mirror plane. Because of the wide field of view, as well as the broad, energy-dependent response of HILT, absolute flux measurements are not possible and are not attempted in this paper.

Launched in September 1991, UARS is in a 585-km altitude, 57° inclination orbit. The High-Energy Particle Spectrometers of the Upper Atmosphere Research Satellite Particle Environment Monitor (UARS/PEM) investigation [*Winningham et al*., 1993] measured electrons in 32 energy channels from 30 keV to several MeV with 4-s time resolution using a set of four sensors with geometric factors of ~0.54 cm^2 sr that provide 30° angular resolution from zenith to the horizon.

The lightning data were acquired with the Optical Transient Detector (OTD), which is on board OrbView-1, a small satellite orbiting at 750 km with a 70° inclination. The OTD is an optical imager that detects and locates lightning activity within its 1300 × 1300 km field of view with 2-ms timing resolution [*Christian et al*., 1999]. Although OTD passes over a given region of Earth only twice per day, it nevertheless provides a good documentation of primary thunderstorm hot spots around the globe on a given day.

3. Significance of the Drift Loss Cone

Because of the low altitudes of SAMPEX and UARS, most of the time when the satellites are on closed magnetic field lines, they also are below the stable trapping region wherein charged particles can repeatedly drift around Earth. In Plate 1 the altitude of the $B = 0.24$ G point along the $L = 1.6$ drift shell is shown for both hemispheres as a function of geographic longitude. A magnetic field magnitude of 0.24 G was chosen for illustration because, for this choice, a minimum altitude of 100 km is just reached in the Southern Hemisphere at a longitude of 330°. An altitude of 100 km is traditionally taken to be the boundary below which energetic particles are lost into the atmosphere. At 100 km the atmospheric density is significant in terms of electron range, and the scale height of atmospheric density here is <20 km, making 100 km a convenient and realistic approximation of the trapping boundary in mirror point altitude. Thus any electron that mirrors at $B = 0.24$ G just reaches 100 km during its drift; any electron that mirrors at a value of $B > 0.24$ G must drop below 100 km and be lost. The key points to be seen in Plate 1 are that for $L = 1.6$ at the SAMPEX and UARS orbital altitudes, (1) no stably trapped particles are ever seen in the Northern Hemisphere; (2) no stably trapped particles are seen in the southern hemisphere between the longitudes of 40° and 290°, well over half the Earth; and (3) only at longitudes where the locus of $B = 0.24$ G drops below the SAMPEX altitude of ~600 km (stippled area in Plate 1) can SAMPEX see trapped particles.

It is clear that for the great majority of the time, SAMPEX and UARS do not observe stably trapped electrons but rather detect electrons destined to be precipitated upon reaching the longitude of the South Atlantic Magnetic Anomaly as a result of their westward drift. In this paper, we consider electron measurements made when SAMPEX was located so as to observe electrons in the drift loss cone. (In Plate 1, only the case of $L = 1.6$ is shown, but the situation is similar for $L < 3$, the region studied in this work.) The advantages of observing electrons in the drift loss cone are that all such electrons must necessarily have been recently scattered into the drift loss cone and that there are no stably trapped particles to obscure the new arrivals by causing background counts in the instruments. Measurements of electrons in the drift loss cone date back to the earliest days of space science; *Vernov et al*. [1965] reported on such measurements made on board 1960λ1 and 1960ρ1.

It is useful to briefly consider how transient, localized precipitation into the drift loss cone would appear as observed on a satellite in the drift loss cone, such as SAMPEX and UARS. In Plate 2 we show a plot similar to Plate 1 for several values of B, the magnetic field on the $L = 1.6$ drift shell. Here we suppose that localized lightning causes strong precipitation (LEP) at a longitude of 100°; the narrow, dark gray vertical bar schematically representing electrons scattered into the drift loss cone and the bounce loss cone into a narrow tube of field lines. In particular, electrons are scattered down to altitudes accessible to SAMPEX and UARS. Electrons that mirror below 100 km are immediately lost, while the other electrons drift to the east and spread out in longitude due to the energy dependence of the drift speed. As the electrons proceed eastward, the band of longitudes populated widens. This characteristic is illustrated schematically as lighter gray bars that get broader as the longitude increases. The time for 150-keV electrons to drift from a longitude of ~100° to their demise at

~300° is ~2 hours. Thus electrons scattered into the drift loss cone over Asia and the western Pacific should survive for a few SAMPEX and UARS orbits and can be sampled several times both north and south of the equator. We have shown in Plate 2 a case where the injection is highly localized in time, and thus there is a single band of electrons injected into the drift loss cone that broadens as the electrons drift eastward. However, storm systems and associated lightning can, in fact, last for many hours and can replenish the drift loss cone near the longitudes of the storm system as the electrons scattered earlier drift off to the east.

In summary, individual lightning discharges within a storm launch nonducted whistler wave packets that pitch angle scatter energetic electrons into the loss cone (both bounce loss cone and drift loss cone) in a localized ionospheric area [*Johnson et al*., 1999]. Those electrons in the bounce loss cone are soon absorbed, leaving electrons in the drift loss cone that mirror (near the altitudes of SAMPEX and UARS) at both ends of the field line while drifting eastward. The energy dependence of the drift velocity spreads out the LEP electrons along the drift shell, causing the electron populations scattered by individual lightning flashes to merge into a continuous shell. What is observed on SAMPEX at a given longitude is the superposition of all electrons in the drift loss cone that have been scattered by multiple individual discharges from different thunderstorms located somewhere west of the satellite position and at both ends of the field line. This situation is observed repeatedly and is described in this paper.

4. Observations

We begin with data from SAMPEX. Plate 3 shows the time history of the count rate of >150 keV electrons from day 95/173 until 95/208 in the interval of $1.3 < L < 2.8$. Data are plotted only if acquired when SAMPEX was in the drift loss cone. The data have been smoothed, and the fine-scale variation with L has been removed. Some daily periodicity still can be seen and is a result of the motion of SAMPEX relative to the boundaries of the drift loss cone and the bounce loss cone. Some of the time, electrons mirroring at the location of SAMPEX are near or in the bounce loss cone so that their lifetimes are a few seconds, and no transient population can persist. At low L values, during a significant fraction of the time, SAMPEX is positioned to detect electrons in the drift loss cone that have lifetimes of tens of minutes. Generally speaking, SAMPEX is well positioned to see such electrons when it is over the Pacific Ocean at low L. It is clear from Plate 3 that >150 keV electrons were frequently scattered into the drift loss cone during this time period, leading to extensive precipitation, especially in the slot region above $L = 2$. Data were routinely collected from the >150 keV electron channel aboard SAMPEX for approximately a year, from July 1994 until August 1995. The precipitation pattern over the entire year period (not shown) exhibits the same general features as that for the limited time period shown in Plate 3.

Plate 4 shows SAMPEX data on three consecutive days (95/196, 95/197, and 95/198) as the satellite proceeded northward over a ground track from west of New Zealand and Hawaii toward Alaska. The precipitation is displayed as color-coded bands on the SAMPEX ground track. In addition, on the right of each geographic plot is a line plot of the same time history of >150 keV electrons. The geographic plots also show as red dots the locations of lightning discharges detected by the OTD during a 3-hour period centered at the equatorial crossing of the SAMPEX passes. The oceanic storm just to the west of the SAMPEX ground track, which was active on 95/197 but not on 95/196, was well placed to generate the observed drift loss cone electrons. The storm of interest in the western Pacific was clearly a large mesoscale convective complex that was long lived, as is evident from its presence for 95/198 in Plate 4, and produced large amounts of lightning, an unusual feature for oceanic storms. Note that the OTD data were acquired within 3 hours of the SAMPEX pass so that the particular lightning flashes shown as red dots most likely would not have occurred during the ~20-min SAMPEX pass shown. The point is that the storm persists over a time period of many orbits, and whistlers launched by lightning discharges within the storm pitch angle scatter electrons for an extended time period. SAMPEX makes passes through regions populated by the electrons in the drift loss cone. Note that electrons in the drift loss cone observed by SAMPEX could well have been scattered tens of minutes earlier because the drift period for ~150 keV electrons in the drift loss cone is ~4 hours (note that the average drift loss cone lifetime is more than 3 orders of magnitude larger than the bounce loss cone lifetime). Plate 4 clearly shows that the electrons in the drift loss cone were observed at similar L shells in geomagnetically conjugate regions and that structured LEP injection into the drift loss cone persisted at least for a few hours.

Plate 5 (top) shows the same SAMPEX ground track and data as shown in Plate 4 (middle) together with two consecutive UARS tracks, one of which shows data taken within the same hour as SAMPEX. These two satellite observations show the global extent of the LEP precipitation, the electrons observed on the UARS orbits to the west of the SAMPEX track likely being due to other thunderstorms (not shown) that were active in southern Malaysia and Sumatra within the same 2-hour period. Note that these electrons would eventually drift east to the position of SAMPEX, as described in Plates 1 and 2.

Also shown is the energy spectrum of the drift loss cone electrons as measured by UARS. The spectrum exhibits a general shape and range (i.e., including electrons with energies between 100 and 200 keV with a broad peak at ~150 keV) strikingly similar to previously documented spectral characteristics of LEP events in the bounce loss cone [e.g., *Voss et al*., 1998, Plate 1]. This similarity lends additional support to the argument that the observed drift loss cone features are produced by the LEP process and not by other sources such as by VLF transmitters, which, due to the nearly monochromatic nature of the signals, have been observed to produce narrow spectral lines whose energy decreases with L [*Imhof et al*., 1981]. Plate 4 (bottom) shows an expanded plot of the SAMPEX data versus L for both the Northern and Southern Hemisphere sections of this orbit; in this case, we show the data taken at a sample rate of one measurement every 30 ms. Both the L shell fine structure and the relative amplitude of the precipitation in the drift loss cone remained remarkably similar during the ~20 min it took SAMPEX to move from the Southern to the Northern Hemisphere. The congruence of the precipitation distribution in both hemispheres is compelling evidence for very localized, strong pitch angle scattering on some L shells into the drift loss cone. The observed congruence is highly unlikely to be due to chance occurrence.

Examination of SAMPEX data during times when the satellite was positioned to detect only those electrons in the drift

loss cone has revealed hundreds of cases of newly enhanced drift loss cone fluxes in localized L shell regions, often associated with individual thunderstorms. The conjugate observations on 95/197 of several sharp peaks at specific L shells are particularly interesting and revealing and are unique in the year of SAMPEX data with high time resolution at ~150 keV. More typically, a single or a single bifurcated peak below $L < 1.9$ is accompanied by a broad peak, often with some structure, filling the slot region. In addition a weak, broad peak is sometimes seen at lower L.

A more typical active day of LEP observations, 95/154, is shown in Plates 6–8. Plate 6 shows the SAMPEX ground track on two consecutive orbits, and Plate 7 shows a greatly expanded display of the sort presented in Plate 1. In Plate 7, each vertical bar is only a quarter of an orbit and only for $L < 4$. Plate 6 is labeled to enable the reader to follow the path of SAMPEX, as shown in Plate 7. Note how the SAMPEX track in L space "weaves" back and forth in Plate 6. A display of the type shown in Plate 6 makes it very easy to find low L conjugacy in the drift loss cone precipitation as well as intermittent low L precipitation.

Plate 8 shows a south-to-north pass on day 95/154 analogous to Plate 5 (bottom) for day 95/197. In this case, we see a broad, weak peak around $L = 1.3$, a relatively narrower peak near $L = 1.7$ and another broader peak near $L = 2.5$. Here again is clear evidence that multiple areas of localized precipitation persisted for at least tens of minutes.

There were a few dozen days in the 1-year period when SAMPEX was operated in the high-resolution mode for relatively lower energy electrons (>150 keV) during which the observations shown in Plate 7 were quite typical. Of course, one would expect great variability from day to day due to the variability of the location, intensity, area, latitude, and longitude of the severe storms generating the lightning. In addition, the intensity of the source population of electrons in the slot region that are scattered by the whistlers is strongly dependent on geomagnetic activity. Nevertheless, the same general characteristics were seen repeatedly.

5. Interpretation of L Dependence

The large spread of nonducted whistler ray paths from a single lightning flash leads to precipitation over a large (~2000 km lateral extent) ionospheric region and an extended range of L shells, often displaced poleward from the source lightning, depending on the particular magnetoplasma gradients [*Lauben et al*., 1999]. It is therefore not easy to uniquely associate the L shells of enhanced fluxes with those of thunderstorms. Nevertheless, both the spatial/temporal association and ray-tracing-based calculations (see below) suggest that the oceanic storm evident on 95/197 in Plate 4, having a substantial north-south extent, is very likely the cause of both the fine structure at $L < 1.8$ and the broad peak between L of ~1.8 and 2.4 (Plate 4). Whistler mode ray paths at the typical few kilohertz frequencies excited by lightning discharges initially traverse the magnetic equatorial plane at relatively low L along a short path to the conjugate hemisphere. The wave is then magnetospherically reflected at the point where the wave frequency is nearly equal to the lower hybrid frequency, and the ray path is directed to substantially higher L shells. Subsequent multiple reflections occur during which the rays are confined to an L shell range characteristic of the signal frequency (~2 to 2.2 for 5 kHz [*Ristic-Djurovic et al*., 1998, Figures 3 and 4]). Thus the narrow low-L peaks may be due to precipitation caused by the first ray paths originating at multiple lightning flashes in different parts of the extended storm (hence the spread in L), while the broad peak may be due to the superposition of the precipitation produced by the multiple reflecting components from lightning discharges originating at different L shells. This qualitative expectation is generally supported by a ray-tracing-based model calculation of the L dependence of the precipitation expected for the case in which a thunderstorm with a finite lightning discharge rate is located at a magnetic latitude $\lambda_m = 25°$ (L ~1.22), as shown in Plate 4.

Plate 9a shows 1 and 5 kHz rays launched at 1000 km altitude at $\lambda_m = 20°$ and $\lambda_m = 30°$, which remain very close to each other until they cross the magnetic equator and quickly disperse upon successive magnetospheric reflections thereafter, with each frequency component eventually settling on a specific L shell. This "focusing" of the ray paths is due largely to the frequency-dependent bending of the rays resulting from the combination of a strong ambient magnetic field, relatively high electron densities, and strong horizontal density gradients. The particular density profile used to produce the result shown was selected from among a range of profiles predicted by the International Reference Ionosphere to be in effect at these low (near-equatorial) latitudes. Consequently, rays injected at different magnetic latitudes cross the magnetic equator in a relatively narrow L shell range of $1.4 < L < 1.5$.

Plate 9b shows the predicted time-integrated precipitated electron flux (>150 keV) due to the pitch angle scattering induced by nonducted whistlers originating in a single lightning discharge. To construct Plate 9b, impulsive waves originating at a lightning discharge at $\lambda_m = 25°$ ($L \sim 1.22$, corresponding to the location of the most pronounced thunderstorm center based on OTD data) were first propagated in the Earth-ionosphere waveguide, where they travel to long distances while continually leaking up (i.e., launching whistler waves upward at latitudes north and south of that of the source lightning) to the magnetosphere along their way. The whistler waves thus launched over a range of latitudes propagate in the nonducted mode over ray paths similar to those shown in Plate 9a. The intensity of the magnetic field component of the whistler wave was computed as a function of space and time using the Stanford VLF two-dimensional ray-tracing code [*Inan and Bell*, 1977]. The effects of Landau damping were included, using the theoretical formulation of *Brinca* [1972] in conjunction with typical suprathermal electron distributions observed by the HYDRA instrument on the Polar space craft [*Bell et al*., 1999]. Each ray was traced until its amplitude was reduced by 3 dB due to Landau damping, after which time it was assumed that the wave-induced precipitation due to the remaining wave energy was negligible. The average intensity of the wave magnetic field as determined as a function of time at every point in space was used to calculate the precipitated flux, assuming it to be proportional to $B_w \nu^2 \gamma^{-4} E^{-3} \nu_\parallel^{-1}$, where B_w is the wave magnetic field intensity, ν is the particle velocity, and γ is the usual relativistic factor. The factor γ^{-4} results from two effects. First, the pitch angle change of the scattered electrons is inversely proportional to the particle mass, and thus Da is proportional to γ^{-1}. Second, the particle flux is specified in terms of counts/keV sr s and the transformation from differential velocity to differential energy introduces an additional factor of γ^{-3}. The factor E^{-3} represents the assumed energy dependence of the electron distribution function, and $\nu_\parallel^{-1}$ accounts for the duration of the resonant interaction. Note that whistler

waves that pitch angle scatter the energetic electrons are inherently coherent, so that the precipitation flux is linearly proportional to the wave amplitude [e.g., *Inan et al*., 1982, Figure 14], rather than B_w^2 as it would be for a diffusion-type process. The wave intensity was calculated for all frequency components over the range 500 Hz to 25 kHz, and precipitated flux contributions were integrated over time to produce the L dependence shown in Plate 9b. It should be noted that what we show in Plate 9a is a rather crude first-order estimate of the precipitated flux, primarily for the purpose of bringing out the L dependence as dictated by the distribution of the whistler mode ray paths shown in Plate 9a. For this purpose, we assume the trapped flux at the edge of the loss cone to be constant with L shell. The trapped flux levels for energetic particles, in fact, exhibit substantial variations with L, but this variation is highly dependent on geomagnetic activity and conditions. Results for any given variation of flux with L can be inferred from Plate 9b since the precipitated flux is linearly proportional to the trapped flux level at the edge of the loss cone [*Inan et al*., 1982].

The predicted energetic electron drift loss cone flux, plotted as a function of L shell, exhibits a broad peak extending from $L = 2$ to $L = 2.5$ and a secondary narrower peak between $L = 1.4$ to 1.5. The broad main peak is produced by high wave normal whistler wave components that undergo multiple reflections in the magnetosphere (as shown in Plate 8a) and scatter electrons over a broad range of L values. The narrow peak is produced by lightning-generated whistlers as they first cross the magnetic equatorial plane (at relatively low L) and before they reflect. The predicted variation of the precipitation with L shell shows the same general form from $1.7 < L < 2.5$ as the SAMPEX observations shown in Plate 5 (bottom). The differences would be due to the latitude of the lightning, to the density gradients in the ionosphere, and to our approximate evaluation of the L dependence of the precipitation flux.

The predicted drift loss cone flux is shown in arbitrary units since it is directly proportional to the unknown lightning discharge rate of the thunderstorm, and our approximate method of estimation only aims at bringing out the L dependence. For typical thunderstorms of 100 km scale the precipitated flux shown in Plate 9b would extend for ~300 km in the east-west direction, centered on the storm. Since thunderstorms are dynamic variable systems, the lightning discharge rate will typically alternate between high and low, and the drift loss cone flux distributions shown in the figures will wax and wane many times during the lifetime of the storms. The drift loss cone flux enhancements typically observed on SAMPEX consist of one or two sharp peaks at $L < 1.8$ followed by a broad peak at $L > 1.8$, quite similar to that shown in Plate 9b. As previously discussed, the 95/197 case shown in Plate 5 (bottom) is unusual, consisting of multiple (or latitudinally extended) thunderstorm centers that remain active to maintain the multiple sharp peaks at $L < 1.8$.

The distribution of whistler mode ray paths as shown in Plate 9a is highly dependent on the cold plasma density distribution. Ray-tracing calculations using different horizontal ionospheric density gradients indicate that the sharp low-L peak shown in Plate 9b is manifested only when the low-latitude ionospheric electron density gradients are such as to focus lightning-generated whistler wave energy at the first equatorial crossing, as shown in Plate 9a. When the horizontal density gradients are such that this type of focusing does not occur, the low L shell peak is wider and may even be completely washed out [*Bortnik et al*., 2000]. Nevertheless, the broad peak above L of ~1.8 is robustly produced under different conditions, being entirely due to the precipitation caused by the whistlers undergoing multiple magnetospheric reflections. The fact that sharp low-L peaks as shown in Plate 9b occur only for a selected range of horizontal density gradients is consistent with the fact that SAMPEX observations of narrow low-L peaks as shown in Plate 4 are rare. Analysis of SAMPEX data from 1995 indicates that the broad peak above L of ~1.8 is commonly observed, with occasional accompanying single narrow low-L peaks.

In a two-dimensional geometry, allowing for only latitudinal density gradients, lightning discharges originating in a given thunderstorm center would produce only one low-L precipitation peak, as shown in Plate 9b. In fact, results indicate that we should refine our qualitative arguments above, associating the multiple narrow peaks to multiple storm centers since lightning flashes originating at different latitudes within a thunderstorm having a north-south extent (e.g., that shown in Plate 4) would still tend to produce a single peak since the primary cause of the narrow peak is the ray path focusing shown in Plate 9a. However, noting that the wave energy from lightning spreads out (in both longitude and latitude) in the Earth-ionosphere wave guide, variations in the latitudinal profile of electron density with longitude can lead to multiple peaks, with the focusing L shell regions being different at different longitudes. In the rare event that many such focusing regions have active storm centers beneath them, a satellite such as SAMPEX would see enhanced sharp precipitation peaks at a variety of low-L locations, each peak being due to a different storm center and focusing region.

6. Discussion

As mentioned in section 1, past observations of LEP bursts in the bounce loss cone on satellites [*Voss et al*., 1998] and on the ground (via the associated D region ionization) indicated that tens to hundreds of LEP events may be produced by a single thunderstorm [e.g., *Inan et al*., 1988a, 1990; *Lev-Tov et al*., 1995]. However, until the recent observation of LEP events produced by nonducted whistlers [*Lauben et al*., 1999; *Johnson et al*., 1999], these events were thought to be produced only by ducted whistlers, which propagate within (and thus affect only the electrons within) filamentary ducts <400 km at the equator [e.g., *Burgess and Inan*, 1993]. Uncertainties in the number and size of ducts made it difficult to estimate global consequences of the LEP phenomenon [*Walt*, 1996; *Voss et al*., 1998]. The observations presented in this paper underscore the role of nonducted whistlers and indicate that the LEP process may be more pervasive than previously thought.

The significance of whistler waves from lightning in the precipitation of energetic electrons was first recognized by *Dungey* [1963]. Using incomplete data on wave characteristics, *Roberts* [1969] argued that precipitation by ducted whistlers led to inconsistent pitch angle distributions, energy spectra, and electron lifetimes. *Kennel and Petschek* [1966] studied the role of whistler mode waves generated by the electrons, while *Lyons et al*. [1972] investigated the effect of plasmaspheric hiss on trapped electrons. Measurements since then have shown that whistler waves from lightning often represent the dominant wave energy in the 0.1–30 kHz range [e.g., *Gurnett and Inan*, 1988] and that individual whistlers can cause significant precipitation as described above. A recent comparative global study of pitch angle scattering by waves from different sources

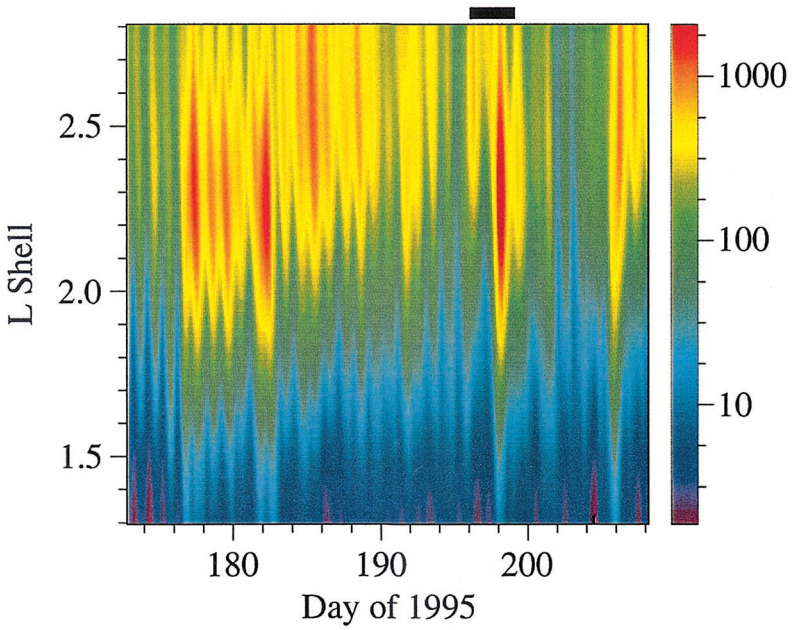

Plate 3. The time history of drift loss cone electrons from 95/173 until 95/208 is shown in a color plot format; substantial temporal variability is seen. The specific time period under discussion in this paper is indicated by the bar at the top.

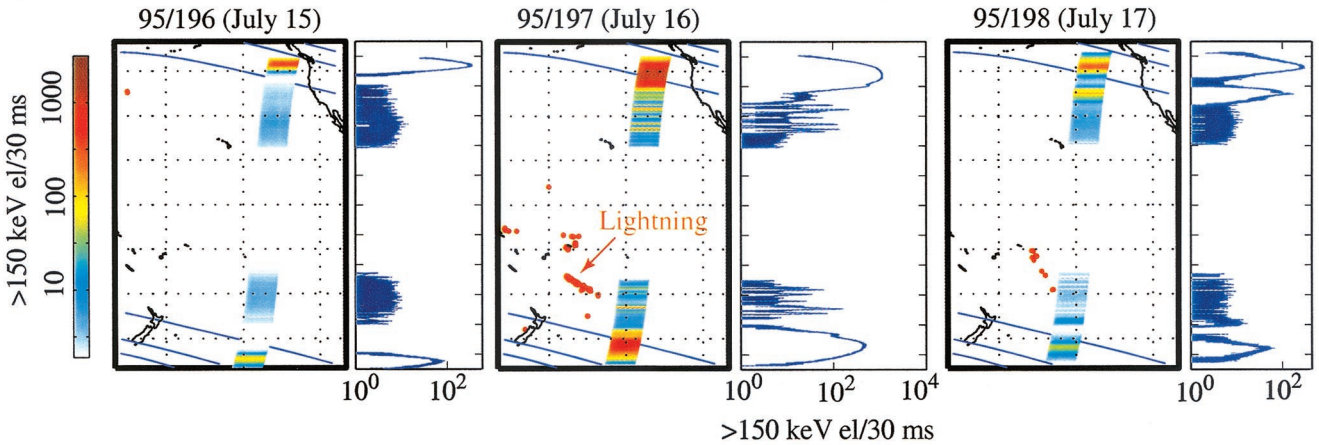

Plate 4. Orbital tracks are shown on three successive days when SAMPEX was northbound between Hawaii and the mainland. Electron intensities are shown in spectrogram format on a map, and as time history line plots. Lightning discharges detected by the Optical Transient Detector are shown as red spots. By about midday of 1995/197, a rather intense oceanic thunderstorm became active in the southern Pacific Ocean, causing substantial drift loss cone LEP enhancements in the range $1.8 < L < 3$ throughout the duration of the thunderstorms.

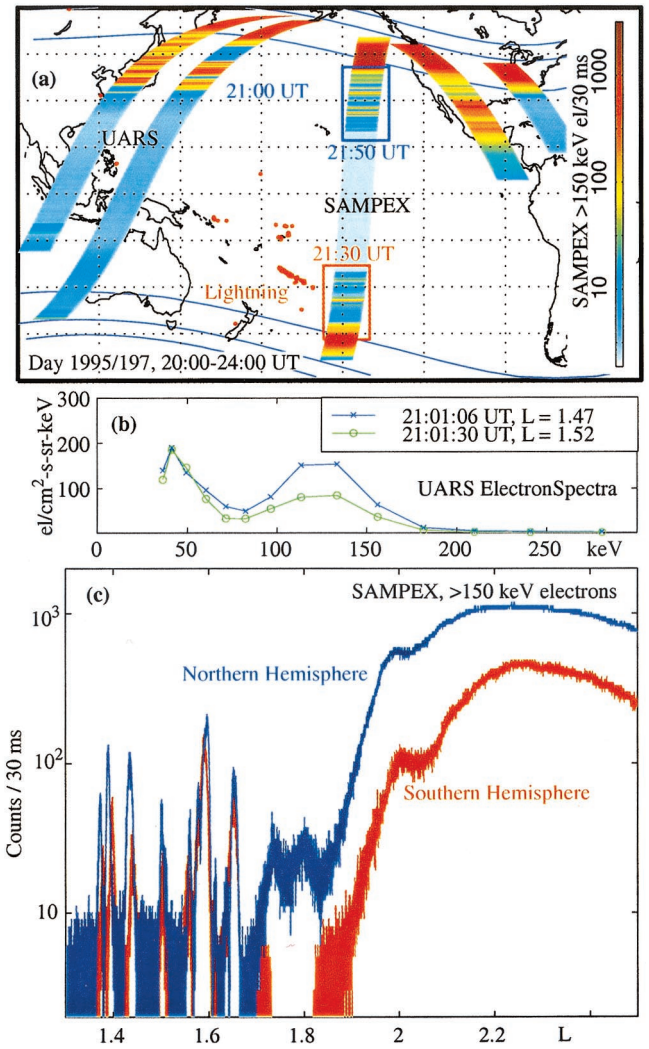

Plate 5. (top) Drift loss cone electrons ($E > 150$ keV) observed on board SAMPEX and UARS ($E > 30$ keV) are plotted in spectrogram format on their orbital tracks. Because both satellites were in the drift loss cone, all of the observed electrons were destined to be precipitated at or before reaching the South Atlantic Magnetic Anomaly. (middle) Electron spectrum, as seen at UARS, is plotted. (bottom) The time history of the electron intensity at SAMPEX is shown, giving unequivocal evidence for the conjugate nature of the drift loss cone electrons.

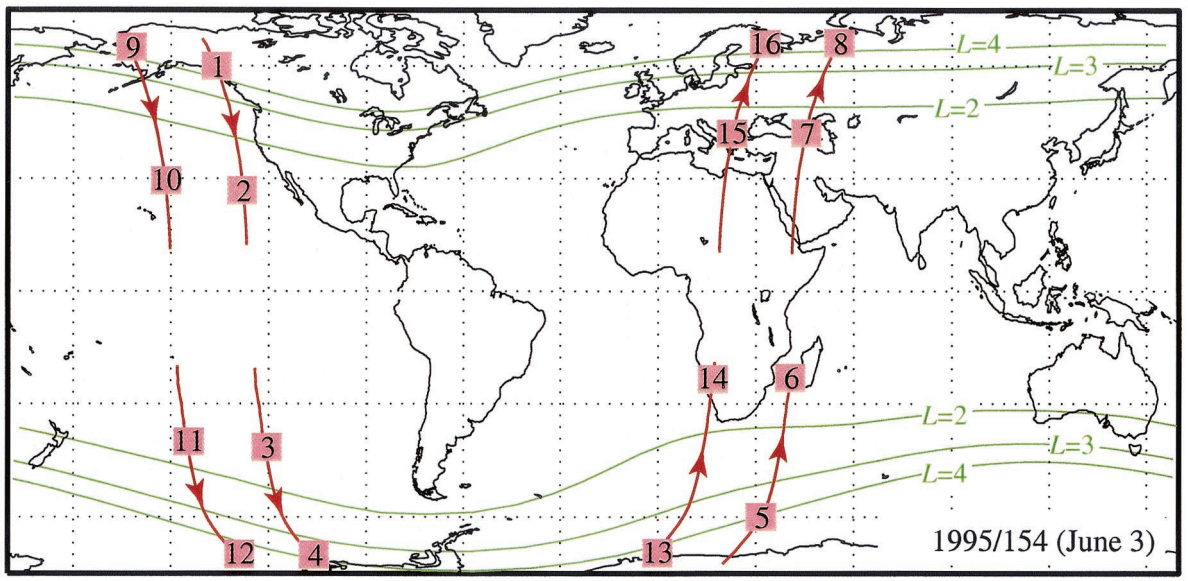

Plate 6. SAMPEX ground track is shown for two consecutive orbits on day 95/154. This plot is to aid in the interpretation of Plate 7.

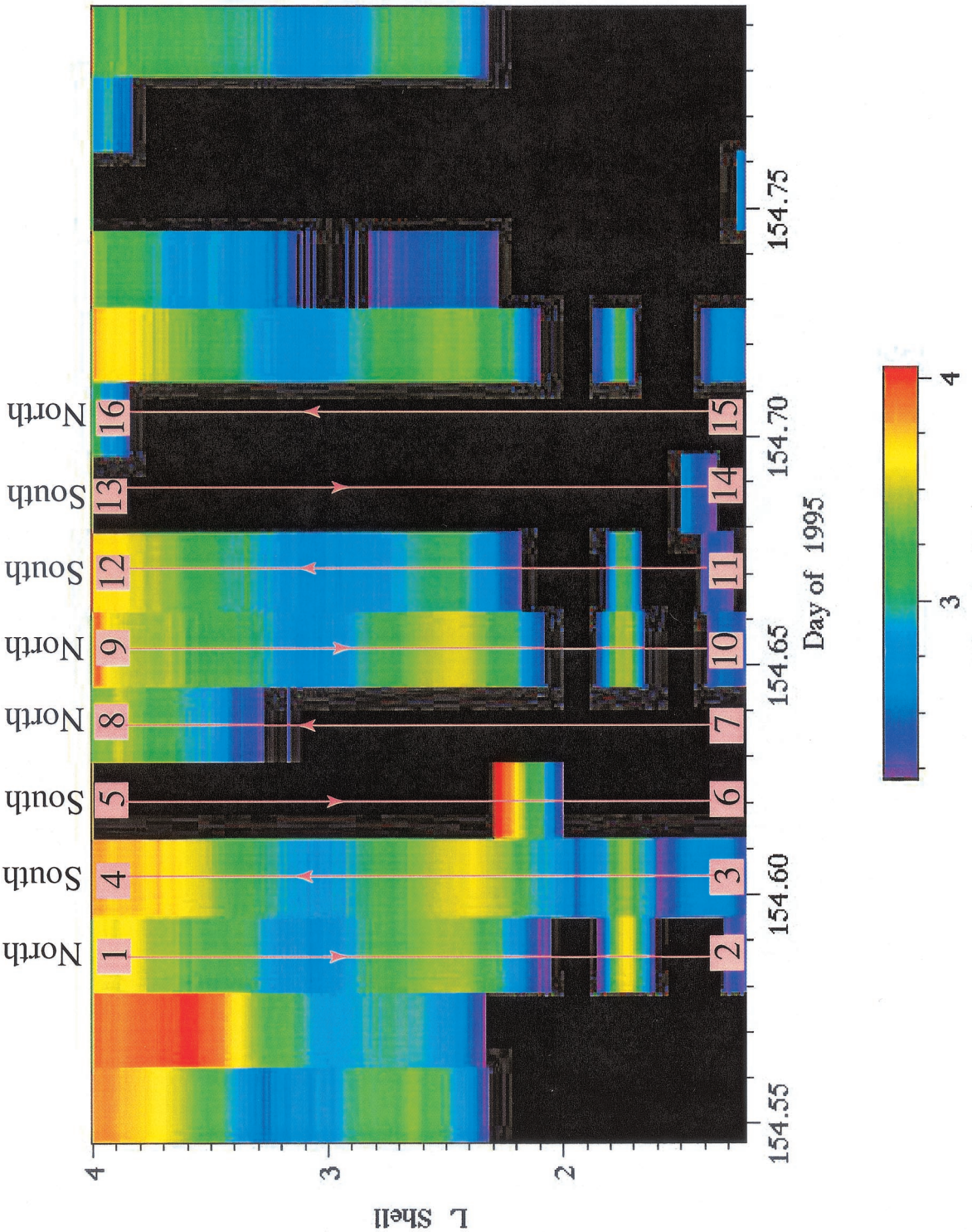

Plate 7. Color plot is shown for SAMPEX drift loss cone measurements on day 95/154. Plots like this one are a compact means of viewing the L dependence of the drift loss cone electron fluxes observed by SAMPEX.

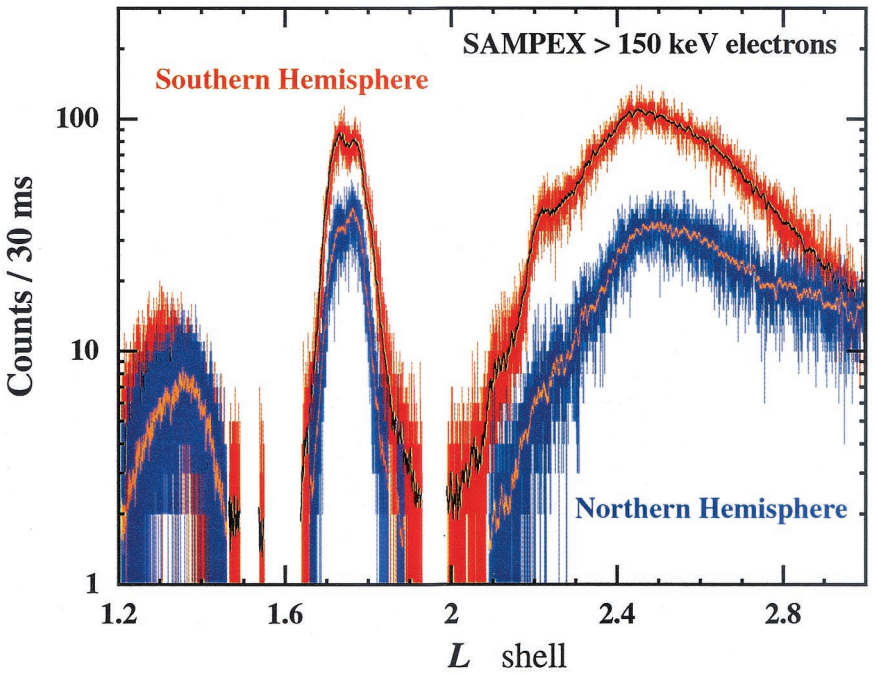

Plate 8. A south-to-north pass of SAMPEX is shown for day 95/154. It is in the same format as the plot shown in Plate 5 (bottom) for day 95/197.

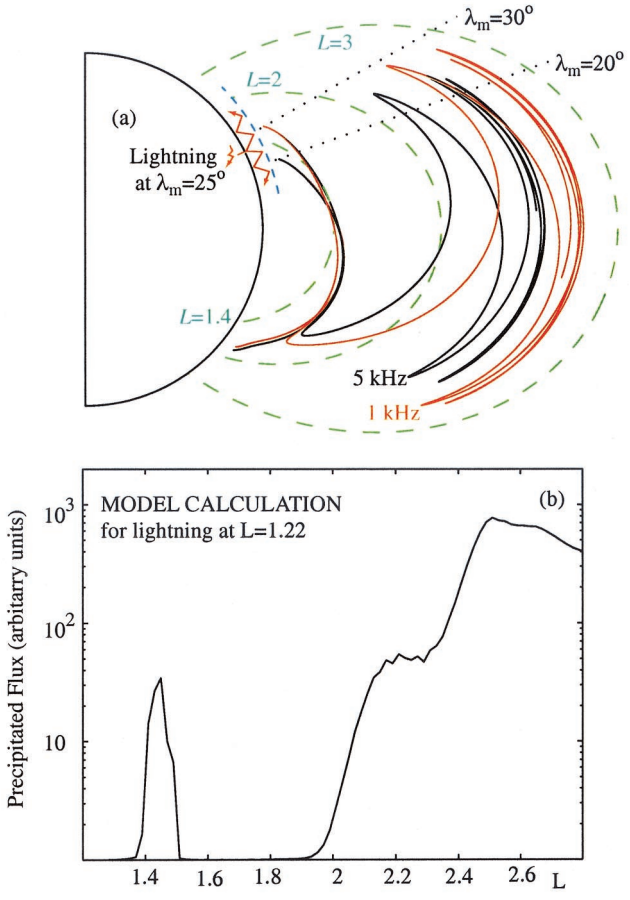

Plate 9. (a) VLF waves originating at lightning discharges spread out (shown only in latitude but, in fact, occurring also in longitude) in the Earth-ionosphere waveguide, continually leaking through the ionosphere to the magnetosphere over a range of latitudes (and longitudes) as shown. Once in the magnetosphere, the VLF rays propagate in accordance with the gradients of the static magnetic field and cold plasma density along ray paths that initially traverse the magnetic equatorial plane at relatively low L along a short path, followed by magnetospheric reflection that directs the ray path to substantially higher L shells and multiple reflections during which the rays are confined to an L shell range characteristic of signal frequency. For particular types of horizontal electron density gradients the ray paths can be focused such that the first crossing of the magnetic equatorial plane occurs in narrow range of L shells. (b) Relative magnitudes as a function of L of the precipitation flux of >150 keV electrons calculated in the manner described in the text. The results are based on the assumption that the flux of the trapped electrons at the edge of the loss cone is constant with L.

[*Abel and Thorne*, 1998a, 1998b] concluded that lightning-produced waves significantly affect the electron belt, especially at $1.8 < L < \sim 2.5$, although this conclusion was also based on ducted whistler occurrence rates. *Abel and Thorne* [1998a, 1998b] also investigated the role of plasmaspheric hiss and VLF transmitters in addition to lightning-generated whistlers. As mentioned above, plasmaspheric hiss has long been suspected to be important in the loss of radiation belt electrons. However, Abel and Thorne indicated that the contributions to radiation belt loss rates by plasmaspheric hiss was negligible for $L < \sim 2.3$. They also showed that VLF transmitters play a significant role, dominantly at $L < \sim 1.8$, but with significant contributions (although less important than that due to lightning-generated whistlers) extending up to $L \sim 2.4$.

A crude first-order estimate of the role of the LEP process can now be made in view of the new determinations of the spatial extent of precipitation regions induced by nonducted whistlers. On the basis of the results of *Lauben et al*. [1999] and *Johnson et al*. [1999] on the spatial extent of nonducted whistler-induced precipitation and assuming a peak precipitated energy flux of $\sim 10^{-2.5}$ ergs cm^{-2}, the fraction of trapped electrons between $L = 2$ and 4 which are precipitated in a single LEP burst is estimated to be $\sim 10^{-6}$. According to *Christian et al*. [1999] the number of nighttime (when ionospheric losses are lower) global lightning flash rate is ~ 35 s^{-1}, and the fraction of lightning discharges at latitudes suitable for LEP is ~5–10%. Using these values, the trapping lifetime for 100–400 keV electrons in this region is estimated to be 3–6 days, comparable to the measured lifetime of 5–10 days [*Schulz and Lanzerotti*, 1974, p. 124–125]. In comparison, lifetimes deduced on the basis of ducted whistler LEP effects alone are much longer [*Walt*, 1996; *Voss et al*., 1998].

7. Summary and Conclusions

Preliminary examination of the 1994 and 1995 SAMPEX data during times when the satellite is positioned to detect only electrons in the drift loss cone has revealed hundreds of cases of enhanced drift loss cone fluxes in localized L shell regions, indicating that the precipitation of electrons with energies of a few hundred keV into the drift loss cone is global and commonplace. Plate 3 shows a month-long period; other times were observed to be very similar. Furthermore, on the basis of the association with lightning (Plate 4), the distinctive energy spectra (Plate 5), and the interpretation of a rather distinctive L dependence dictated by nonducted whistler mode ray paths (Plate 9), this precipitation is apparently driven by whistler waves originating in thunderstorms active around the globe at any given time.

Acknowledgments. This work was supported by NASA at The Aerospace Corporation under NASA Cooperative Agreement 26979B and at Stanford University under NASA grants NAGW-5156 and NAG5-8040. We thank Nikolai Lehtinen for preparing Plates 4 and 5. The Lockheed-Martin work was supported by the Internal Research and Development Program. UARS/HEPS was designed and developed at LMATC under an SWRI subcontract 17167 to NASA contract NAS5-27752.

Janet G. Luhmann thanks Hank D. Voss and another referee for their assistance in evaluating this paper.

References

Abel, B., and R. M. Thorne, Electron scattering loss in Earth's inner magnetosphere, 1, Dominant physical processes, *J. Geophys. Res*., *103*, 2385, 1998a.

Abel, B., and R. M. Thorne, Electron scattering loss in Earth's inner magnetosphere, 2, Sensitivity to model parameters, *J. Geophys. Res*., *103*, 2397, 1998b.

Bell, T. F., U. S. Inan, and J. D. Scudder, Landau damping rates of magnetospherically reflected whistlers determined from PWI and HYDRA observations on POLAR, *Eos Trans. AGU*, *80*(46), Fall Meet. Suppl., F853, 1999.

Bortnik, J., U. S. Inan, T. F. Bell, and J. B. Blake, L-dependence of electron precipitation driven by oblique whistler waves permeating the inner belt, *Eos Trans. AGU*, *81*(48), Fall Meet. Suppl., Abstract SM12A-23, 2000.

Brinca, A. L., On the stability of obliquely propagating whistlers, *J. Geophys. Res*., *77*, 3495, 1972.

Burgess, W. C., and U. S. Inan, The role of ducted whistlers in the precipitation loss and equilibrium flux of radiation belt electrons, *J. Geophys. Res*., *98*, 15,643, 1993.

Christian, H. J., et al., Global frequency and distribution of lightning as observed by the Optical Transient Detector (OTD), in *Proceedings of the 11th International Conference on Atmospheric Electricity*, edited by H. J. Christian, *NASA Conf. Publ*., *1999–209261*, 726–729, 1999.

Dungey, J. W., Loss of Van Allen electrons due to whistlers, *Planet. Space Sci*., *11*, 591, 1963.

Gurnett, D. A., and U. S. Inan, Plasma wave observations with the Dynamics Explorer 1 spacecraft, *Rev. Geophys*., *26*, 285, 1988.

Imhof, W. L., R. R. Anderson, J. B. Reagan, and E. E. Gaines, The significance of VLF transmitters in the precipitation of inner belt electrons, *J. Geophys. Res*., *86*, 11,225, 1981.

Inan, U. S., and T. F. Bell, The plasmapause as a VLF wave guide, *J. Geophys. Res*., *82*, 2819, 1977.

Inan, U. S., T. F. Bell, and H. C. Chang, Particle precipitation induced by short-duration VLF waves in the magnetosphere, *J. Geophys. Res*., *87*, 6243, 1982.

Inan, U. S., D. C. Shafer, W. Y. Yip, and R. E. Orville, Subionospheric VLF signatures of nighttime D region perturbations in the vicinity of lightning discharges, *J. Geophys. Res*., *93*, 11,455, 1988a.

Inan, U. S., T. G. Wolf, and D. L. Carpenter, Geographic distribution of lightning-induced electron precipitation observed as VLF/LF perturbation events, *J. Geophys. Res*., *93*, 9841, 1988b.

Inan, U. S., F. A. Knifsend, and J. Oh, Subionospheric VLF imaging of lightning-induced electron precipitation from the magnetosphere, *J. Geophys. Res*., *95*, 17,217, 1990.

Johnson, M. P., U. S. Inan, and D. S. Lauben, Subionospheric VLF signatures of oblique (nonducted) whistler-induced precipitation, *Geophys. Res. Lett*., *26*, 3569, 1999.

Kennel, C. F., and H. E. Petschek, Limit on stably trapped particle fluxes, *J. Geophys. Res*., *71*, 1, 1966.

Klecker, B., et al., HILT: A heavy ion large area proportional counter telescope for solar and anomalous cosmic rays, *IEEE Trans. Geosci. Remote Sens*., *31*, 542, 1993.

Lauben, D. S., U. S. Inan, and T. F. Bell, Poleward-displaced electron precipitation from lightning-generated oblique whistlers, *Geophys. Res. Lett*., *26*, 2633, 1999.

Lev-Tov, S. J., U. S. Inan, and T. F. Bell, Altitude profiles of localized D region density disturbances produced in lightning-induced electron precipitation events, *J. Geophys. Res*., *100*, 21,375, 1995.

Lyons, L. R., R. M. Thorne, and C. F. Kennel, Pitch-angle diffusion of radiation belt electrons within the plasmasphere, *J. Geophys. Res*., *77*, 3455, 1972.

Ristic-Djurovic, J. L., T. F. Bell, and U. S. Inan, Precipitation of radiation belt electrons by magnetospherically reflected whistlers, *J. Geophys. Res*., *103*, 9249, 1998.

Roberts, C. S., Pitch-angle diffusion of electrons in the magnetosphere, *Rev. Geophys*., *7*, 305, 1969.

Roederer, J. G., *Dynamics of Geomagnetically Trapped Radiation*, Vol. 2, *Physics and Chemistry in Space*, Springer-Verlag, New York, 1970.

Schulz, M., and L. J. Lanzerotti, *Particle Diffusion in the Radiation Belts*, *Phys. Chem. Space*, vol. 7, p. 124, Springer-Verlag, New York, 1974.

Vernov, S. N., I. A. Savenko, L. V. Tverskaya, B. A. Tverskoy, and P. I. Shavrin, On the asymmetry of the intensity of fast electron in conjugate points at low altitudes, in *Advances in Space Research*, vol. IV, p. 392, MacMillan, Old Tappan, N. J., 1965.

Voss, H. D., W. L. Imhof, J. Mobilia, E. E. Gaines, M. Walt, U. S. Inan, R. A. Helliwell, D. L. Carpenter, J. P. Katsufrakis, and H. C. Chang, Lightning-induced electron precipitation, *Nature*, *312*, 740, 1984.

Voss, H. D., M. Walt, W. L. Imhof, J. Mobilia, and U. S. Inan, Satellite observations of lightning-induced electron precipitation, *J. Geophys. Res*., *103*, 11,725, 1998.

Walt, M., Source and loss processes for radiation belt particles, in *Radiation Belts: Models and Standards*, Geophys. Monogr. Ser., vol. 97, p. 1, edited by J. F. Lemaire, D. Heynderickx, and D. N. Baker, AGU, Washington, D. C., 1966.

Winningham, J. D., et al., The UARS particle environment monitor, *J. Geophys. Res*., *98*, 10,649, 1993.

T. F. Bell and M. Walt, STARLab, Electrical Engineering Department, Stanford University, Durand 315, Stanford, CA 94305, USA. (bell@nova.stanford.edu; walt@nova.stanford.edu)

J. B. Blake, Space Sciences Department, The Aerospace Corporation, Box 92957, M2/259, Los Angeles, CA 90009, USA. (JBernard.Blake@aero.org)

J. Bortnik and U. S. Inan, STARLab, Electrical Engineering Department, Stanford University, Packard Building, Room 355, 350 Serra Mall, Stanford, CA 94305-9515, USA. (inan@nova.stanford.edu)

D. L. Chenette, Lockheed-Martin Advanced Technology Center, O/H1-11 B/255, 3251 Hanover Street, Palo Alto, CA 94304-1191, USA. (chenette@spasci.com)

H. J. Christian, NASA Marshall Space Flight Center, Huntsville, AL 35812, USA. (Hugh.Christian@msfc.nasa.gov)

(Received March 4, 2001; revised May 17, 2001;
accepted May 17, 2001.)